JPE 16-6-20

http://dx.doi.org/10.6113/JPE.2016.16.6.2192
ISSN(Print): 1598-2092 / ISSN(Online): 2093-4718

Power Management of Open Winding PM Synchronous Generator for Unbalanced Voltage Conditions

Ashraf EL- Bardawil[†] and Mona Fouad Moussa[*]

[†,*]Electrical Power & Control, Arab Academy for Science, Technology, and Maritime Transport, Cairo, Egypt

Abstract

Wind energy is currently the fastest-growing electricity source worldwide. The cost efficiency of wind generators must be high because these generators have to compete with other energy sources. In this paper, a system that utilizes an open-winding permanent-magnet synchronous generator is studied for wind-energy generation. The proposed system controls generated power through an auxiliary voltage source inverter. The VA rating of the auxiliary inverter is only a fraction of the system-rated power. An adjusted control system, which consists of two main parts, is implemented to control the generator power and the grid-side converter. This paper introduces a study on the effect of unbalanced voltages for the wind-generation system. The proposed system is designed and simulated using MATLAB/Simulink software. Theoretical and experimental results verify the validity of the proposed system to achieve the power management requirements for balanced and unbalanced voltage conditions of the grid.

Key words: Permanent magnet synchronous generator, Power management, Static series synchronous compensator, Unbalanced voltage, Wind energy

I. INTRODUCTION

Wind generators must meet any load requirements and produce energy at the minimum investment cost. In wind power applications, more attention is being focused on synchronous generators, particularly permanent magnet types. Permanent-magnet synchronous generators (PMSGs) have the advantages of high efficiency and power density. Moreover, PMSGs with high pole numbers reduce the maintenance cost of wind farms because of their ability to enable direct-drive wind turbines that can eliminate the gearbox. By contrast, to decouple the line frequency and the rotor speed, a full power rating converter is required because synchronous speed is essential for generating power by the PMSG. Wind power systems that utilize PMSGs commonly use a back-to-back PWM voltage-source converter (VSC). Generator efficiency and utilization can be maximized by controlling the generator current with the machine-side PWM VSC. The PWM converter at the grid side provides the grid with controllable real and reactive powers. The system ability and power quality can be improved, but the high cost of the full-rating active power electronic converter is the only disadvantage of this system [1]. Replacing the generator-side PWM VSI with a low-cost diode rectifier has been proposed to reduce the cost of the overall system [2]-[6]. Power conversion technology uses the magnetic energy recovery switch (MERS) to improve output power and efficiency [7], [8]. A DC/DC boost converter must be sized based on the full power rating of the system. However, cost reduction is limited because of the possible need for a high power inductor. The generator also suffers from underutilization issues when operating in a diode rectifier wind power system. A simplified non-salient PMSG model can explain the generator underutilization issue of diode rectifier generating systems. The displacement power factor is unity when the diode rectifier is used. Reducing the terminal voltage applied to the generator can enable the DC/DC boost converter to increase the generator current. The generator power, however, may not increase along with the increase of the generator current. At the same time, the generator current vector will always lag at the back EMF, leading to an inability to deliver

Manuscript received Feb. 14, 2016; accepted Jul. 27, 2016
Recommended for publication by Associate Editor Gaolin Wang.
[†]Corresponding Author: Eng__ashraf@aast.edu
Tel: +2-01062079555, AASTMT
[*]Electrical Power & Control, Arab Academy for Science, Technology, and Maritime Transport, Egypt

the rated power at the rated generator current and voltage [1]. Maximum power point tracking (MPPT) is one of the inherent characteristics of a variable speed wind turbine generator for the optimal operation of wind power systems [9], [10].

On the other hand, the power management control strategy for wind energy systems depends on controlling both active and reactive powers [11], [12]. The advancement of power electronics provides control flexibility. The grid-connected wind power system is used to transfer power to the grid; however, the grid voltage is balanced or unbalanced. Moreover, an unbalanced voltage on the power system causes double-frequency power oscillation at the output power, as reflected by the ripple in the DC bus voltage [13], [14]. In certain cases, these oscillations lead to instability if the DC bus voltage surpasses the most extreme limit. In general, the unbalanced voltage problem can be compensated using a series active power filter by injecting a negative sequence voltage [15], [16], a shunt active power filter by injecting a negative sequence current [17], [18], and series parallel compensators such as the unified power quality conditioners [19], [20].

The present paper discusses an open-winding PMSG with an uncontrolled diode rectifier and an auxiliary fractional-sized compensating VSI. The output power and generator current are improved compared with those in the case of conventional diode rectifiers. In addition, the effects of balanced and unbalanced grid voltages for the system are obtained to achieve power management requirements. The overall system is modeled and simulated using MATLAB/Simulink software and verified by experimental work. The paper is organized as follows. Section I is the Introduction, Section II presents the Proposed Topology and Operating Principle, Section III discusses the Control Method, Section IV explains the Simulation Study, Section V is the Experimental Work, and Section VI is the Conclusion.

II. Proposed Topology and Operating Principle

An open-winding PMSG is used with an uncontrolled rectifier and an auxiliary fractional-sized compensating VSI, as shown in Fig. 1. To understand how the power can be managed from the generator side to the grid side, consider the conventional D-Q model of the IPMSG below [21]:

$$V_d = R_a I_d + p\varphi_d - \varphi_q \omega_e \quad (1)$$

$$V_q = R_a I_q + p\varphi_q + \varphi_d \omega_e \quad (2)$$

$$\varphi_q = L_q I_q \quad (3)$$

$$\varphi_d = L_d I_d + \varphi_f \quad (4)$$

where (V_d, V_q) are the *d*- and *q*-axis components of the stator voltages, R_a is the generator resistance, (I_d,I_q) are the *d*- and *q*-axis components of the stator currents, (L_q, L_d) are the *d*- and *q*-axis components of inductance, φ_f is the amplitude of the flux linkages established by the permanent magnet, p is the operator for differentiation, ω_e is the electrical angular frequency, and (φ_d, φ_q) are the *d*- and *q*-axis components of the flux linkages. In case the three-phase grid voltages possess constant amplitude and frequency, V_d and V_q are constant. Therefore, the active and reactive powers injected into the grid side in the d–q reference frame can be expressed accordingly [22]:

$$P_{grid} = \frac{3}{2}\left(V_{dgrid} I_{dgrid} + V_{qgrid} I_{qgrid}\right) \quad (5)$$

$$Q_{grid} = \frac{3}{2}\left(V_{qgrid} I_{dgrid} + V_{dgrid} I_{qgrid}\right) \quad (6)$$

where P_{grid} and Q_{grid} are the active and reactive powers injected to the grid. The *dq* transformations can be used to align the *d*-axis of the synchronous frame with the grid voltage vector. Therefore, the *q*-axis grid voltage, V_{qgrid} is equal to its magnitude, and the resultant *d*-axis voltage V_{dgrid} is equal to zero. Consequently, the active and reactive powers will be as follows [23]:

$$P_{grid} = \frac{3}{2} V_{qgrid} I_{qgrid} \quad (7)$$

$$Q_{grid} = \frac{3}{2} V_{qgrid} I_{dgrid} \quad (8)$$

The power transferred via the DC link should be equal to the power fed into the grid. Therefore [23],

$$\frac{3}{2}\left(V_{qgrid} I_{qgrid}\right) = V_{dc}\ I_{dc} \quad (9)$$

These equations indicate that the active power infused to the grid can be controlled via the quadrature current I_{qgrid}, whereas the reactive power infused to the grid is accordingly controlled via the control of I_{dgrid}. Thus, the *d*-axis current reference should be set to zero to acquire the unit power factor.

To achieve this goal, the assistant inverter is used for generator control and utilization improvement. The auxiliary inverter is a series compensation device identical to the static series synchronous compensation and can be controlled as a variable three-phase impedance. By contrast, the whole system can be represented by the simple equivalent circuit shown in Fig. 2, in which the AC side voltage of the diode rectifier V_{rect} is equivalent to the vector sum of the generator voltage V_s and the compensation voltage V_{sc}. The inverter is equivalent to a three-phase inductor if the injected voltage is leading the generator current by 90°. When the injected voltage lags the current by 90°, the inverter is effectively a three-phase capacitor. The DC bus of the assistant inverter is basically a DC capacitor that is not associated with a power source, meaning that the inverter can be used to control the compensation DC bus voltage, which is expanded at the point when the injected voltage possesses a component in phase with the current. When the injected voltage is 180° from the current, the compensation DC bus

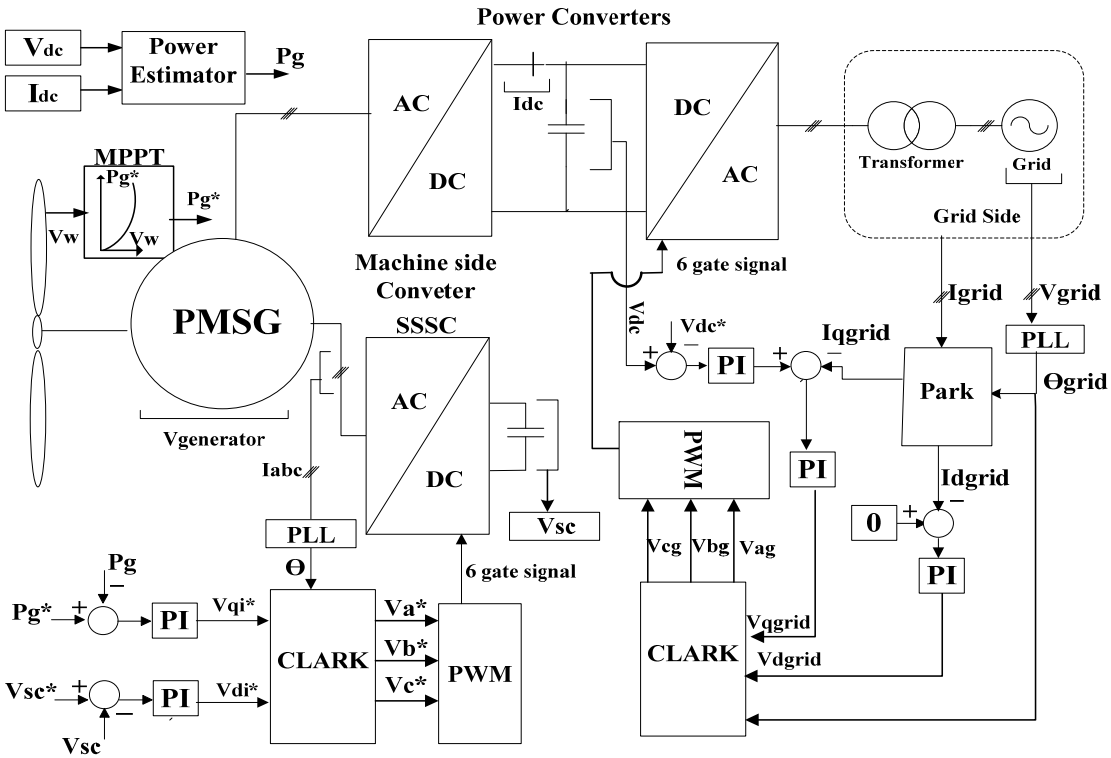

Fig. 1. Proposed control system with wind energy system.

voltage is decreased. Thus, by neglecting the generator resistance and its compensation, the generator is assumed to be purely reactive. The total power flow into the rectifier can be evaluated according to Equation [1]:

$$P_{gen} = \frac{3\,E\,V_{rect}}{X_s}\sin\delta + \frac{3\,V_{sc}\,V_{rect}}{X_s}\sin\varphi_{sc} \quad (10)$$

where P_{gen} is the generator power, E is the generator back-EMF, δ is the power angle defined from the back-EMF E to the rectifier voltage V_{rect}, and φ_{sc} is the angle defined from the compensator voltage V_{sc} to the rectifier voltage. The generated power can be controlled by changing the compensation voltage. If the current is in phase with the voltage, then the rectifier operates at the unity displacement power factor. The generator works on its most extreme torque per ampere curve when the compensation voltage wipes out the voltage drop on the synchronous reactance. The generator power decreases when the compensation is inductive, whereas the generator power increases when the compensation is capacitive.

MPPT algorithms are utilized in wind power systems to convert variable voltage and frequency output to a fixed frequency and fixed voltage output. For example, in the optimum relationship-based control technique, the optimum relationship between the rectifier output voltage V_{dc} and the dc-power P_{dc} is recorded for different wind speeds. The I_{dc}^{*} values corresponding to the maximum power are extracted from the V_{dc} versus P_{dc} relationship.

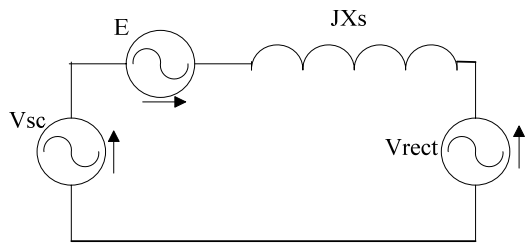

Fig. 2. Series compensation equivalent circuit.

III. CONTROL METHOD

In the proposed system, the control of the grid-side converter is the same as the other topologies using standard active front-end configurations. The control of the generator compensation VSI is examined here because the diode rectifier is not controllable. The proposed control strategy utilizes this idea [1] and examines the performance of power management requirements under both balanced and unbalanced grid voltages using the estimated generator power as the control variable in both cases [1]. The expected source of the imbalance on the grid could be a sudden voltage dip on the single phase of the grid. This study aims to examine whether the control strategy manages power injection to the grid under this transient condition.

As shown in Fig. 1, the controller of the compensation VSI is in the synchronous frame fixed to the generator current, that is, the q-axis is aligned with the peak of phase "A"

TABLE I
PARAMETERS OF PMSG

Parameter	Description	Value
F_r	Rated frequency	30
N_r	Rated speed	900
P	Number of poles	4
L_d	d-axis inductance	0.3
L_q	q-axis inductance	0.37
R_a	Stator resistance	2
h_f	Permanent flux linkage	0.8
L	Smooth inductor	311 mH
R	Internal resistance	21 Ω

current. The two orthogonal components of the compensation inverter voltage, V_{di}, V_{qi}, control the real and reactive powers of the compensation VSI. The components of the VSI voltage V_{di} are utilized to control the floating capacitor voltage. This converter should be designed to exclusively provide reactive power. The only power needed is approximately 5% of its rated KVA to address losses in the devices. As previously mentioned, this power is extremely small compared with the KVA rating of the converter. Another PI controller is used to control the generator power by changing the reactive component of the VSI voltage [1]. The generator power is estimated using the measured current and the main DC bus voltage. The most common synchronization algorithm for extracting the phase angle of the grid voltages is the phase locked loop, which can produce the angle needed in the park transformation from the abc to dq0 synchronous reference frames.

IV. SIMULATION STUDY

The developed system contains an open winding generator with a rated phase voltage of 220 V. All generator parameters are given in Table I. The system contains two power electronic converters. The first converter produced two control input command signals, namely, compensator voltage (V_{sc}) and generator power (P_{gen}). Series compensation devices are used to counter the voltage drop on the synchronous reactance of the generator. These devices are controlled in the impedance mode. The other converter is the grid-side converter, which has been controlled similarly to the other topologies to regulate two control command inputs, I_{qgrid} and V_{dc}, such that I_{dgrid} equals zero-to-zero reactive power injection, thus achieving a unity power factor. On the contrary, V_{dc} provides the means for controlling the active grid current at the unity power factor. The DC-link voltage controller is designed to balance the power flow into the grid.

The flowchart of the simulation study is shown in Fig. 3. The figure clearly illustrates that power management for the balanced grid voltage was achieved. However, the effect of the unbalanced grid voltage on the active and reactive powers injected to the grid still requires further study.

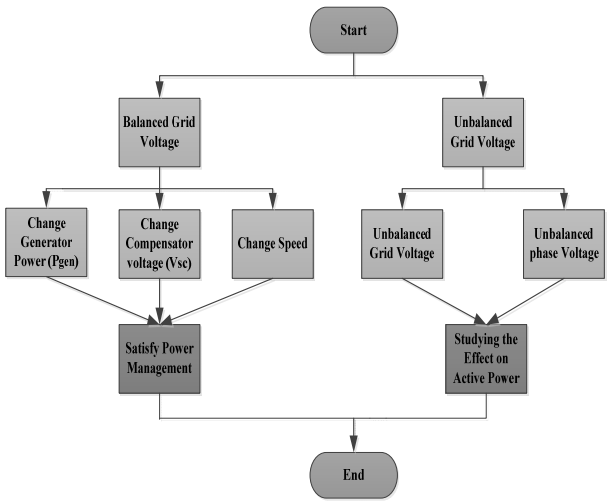

Fig. 3. Flowchart of simulation study.

TABLE II
COMPARISON BETWEEN CONVENTIONAL AND PROPOSED STRUCTURES

Configuration	Conventional s tructure	Proposed structure (Open winding)
Control DC - side	No control on the generator side	Control of the generator-side DC voltage through the auxiliary inverter
Weight	Light	Heavy (auxiliary inverter)
Cost	Low	High
Generator size	Same	Same
Efficiency	Low	5% increase
Configuration	**Conventional s tructure**	**Proposed structure (Open winding)**
Grid inverter	Controls the total power	Auxiliary inverter controls only 15%–25% of the total power
DC-link ripple	2.4	1
Total harmonic distortion	16.2%	5.6%
Grid voltage	110	110

A. Balanced Grid Voltage

In this case, the grid voltages are balanced, and the system is tested under different conditions of input required power, input compensated voltage, and speed.

1) V_{sc} *is kept constant at 100 V, and the speed is maintained at 900 rpm, whereas* P_{gen} *is increased from 750 W to 1500 W at 0.5 s.*

Figs. 4 to 10 show the machine performance before and after the step change of the input power. Figs. 4 and 5 clearly indicate that (V_{sc}) and (P_{gen}) are fully controlled and follow the command value. Figs. 6 and 7 reveal that both actual values of (I_{dgrid}) and (I_{qgrid}) respond to their command value. Both the active and reactive powers injected into the grid are shown in Fig. 8. The component of reactive power is equal to zero, which means the developed system satisfies the power management requirements. Fig. 9 illustrates the

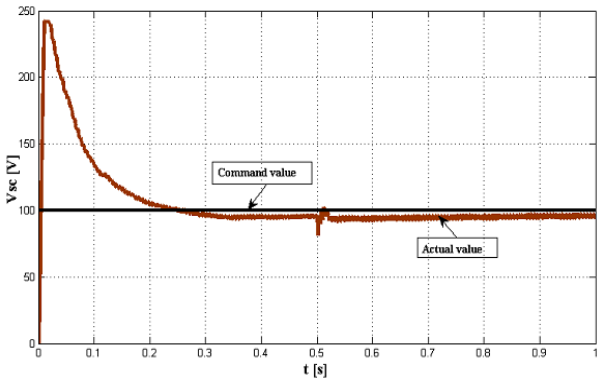

Fig. 4. Compensator voltage (V_{sc}) for the step change in generator power.

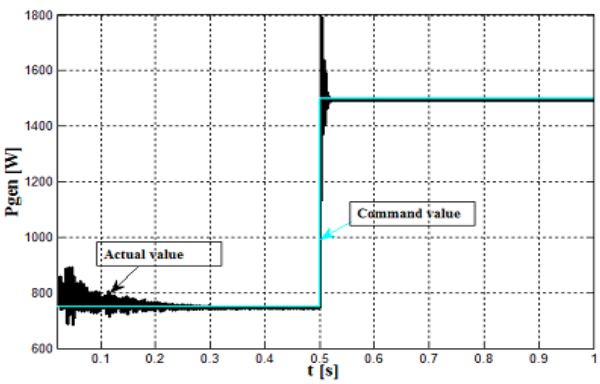

Fig. 5. Generator power (P_{gen}).

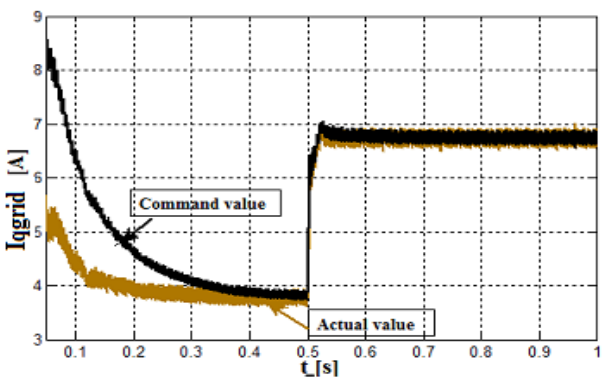

Fig. 6. Quadratic current (I_q) for the step change in generator power.

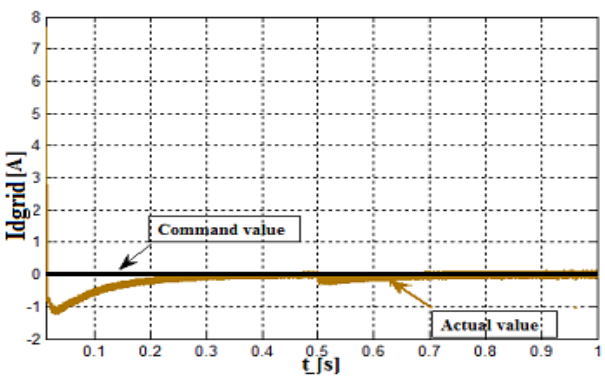

Fig. 7. Direct current (I_d) for the step change in generator power.

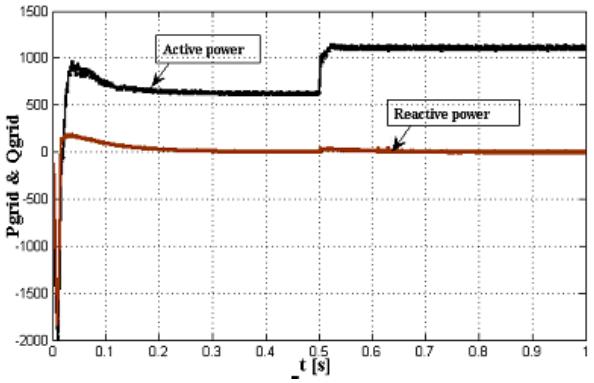

Fig. 8. Active and reactive powers injected to the grid for the step change in generator power.

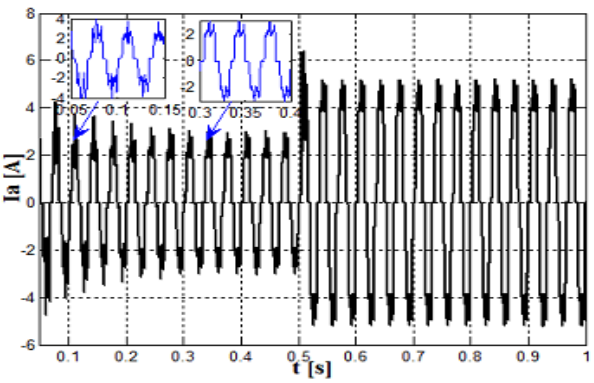

Fig. 9. Generator phase current for the step change in generator power.

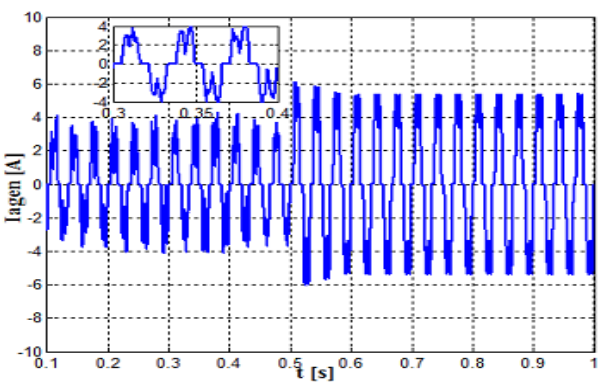

Fig. 10. Uncompensated current for the step change in generator power.

generator current, which generally shows that the generator current is almost smooth and indicated a decreased torque ripple. Fig. 10 shows the uncompensated generator current for the step change in generator power. Tables II show the comparison between the conventional and proposed structures.

2) P_{gen} is kept constant at 1500 W, and the speed is maintained at 900 rpm, while the compensator voltage V_{sc} *is decreased from 100 V to 50 V at 0.5 s.*

Figs. 11 to 15 illustrate the machine performance before and after the step change of the compensation voltage. Figs. 11 and 12 show the performance of the compensator voltage

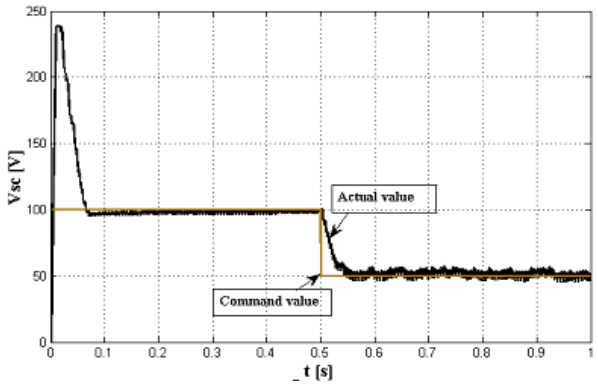

Fig. 11. Compensator voltage (V_{sc}).

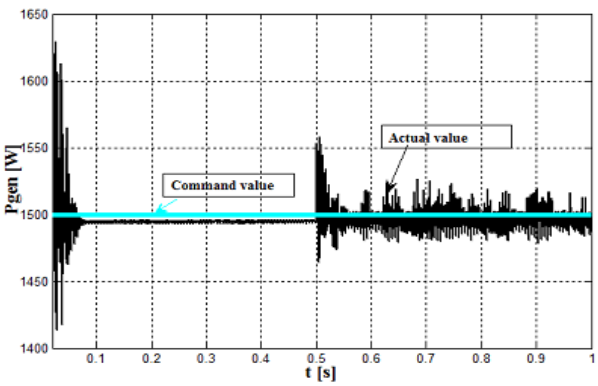

Fig. 12. Generator power (P_{gen}) for the step change in compensation voltage.

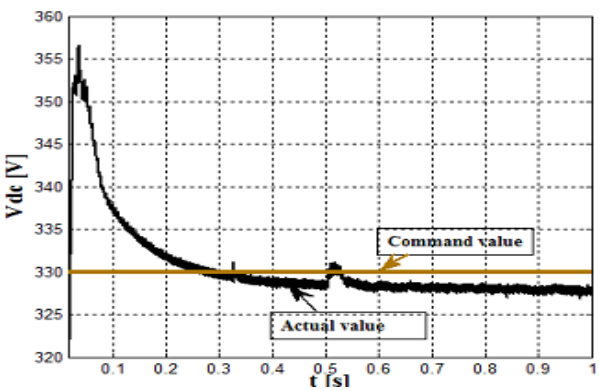

Fig. 13. Rectification voltage (V_{dc}) for the step change in compensation voltage.

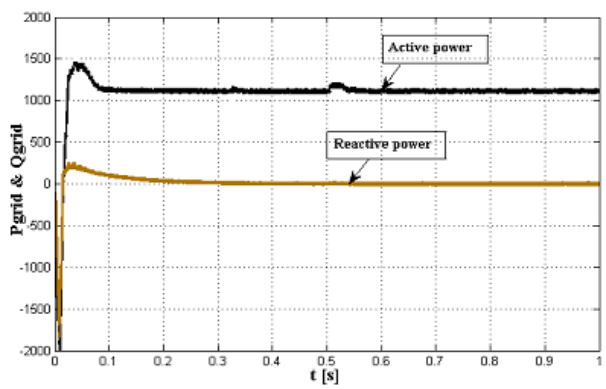

Fig. 14. Active and reactive powers injected to the grid for the step change in compensation voltage.

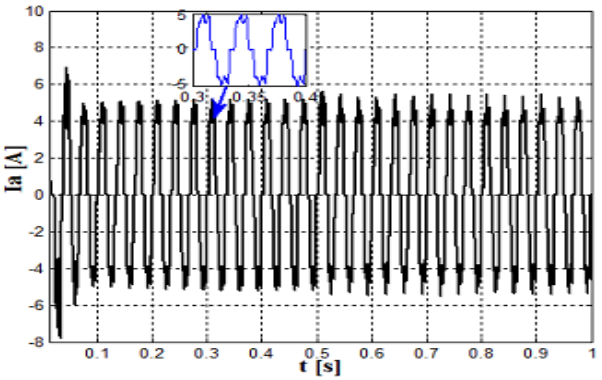

Fig. 15. Generator current for the step change in compensation voltage.

V_{sc} and the generator power P_{gen}; notably, both actual values of V_{sc} and P_{gen} respond to their command values. As indicated in Fig. 13, the actual value of (V_{dc}) follows the command value. Both the active and reactive powers injected into the grid are shown in Fig. 14. Fig. 15 shows the generator current waveform before and after the step change of the compensation voltage, denoting that the current remains constant.

3) P_{gen} is kept constant at 1500 W, and V_{sc} is at 100 V, whereas the speed is changed from 900 rpm to 1050 rpm at 0.5 s.

Figs. 16 to 19 represent the machine performance before and after the step change in speed. Figs. 16 and 17 show the performance of the compensator voltage V_{sc} and the generator power P_{gen}. Both actual values of V_{sc} and P_{gen} follow the command values. The active and reactive powers injected into the grid are shown in Fig. 18. Fig. 19 shows the generator current waveform before and after the step change of the speed. Notably, the current frequency changed from 30 Hz to 35 Hz.

B. Unbalanced Grid Voltage

As for the unbalanced grid voltage, power management was studied by changing the grid voltage as follows.

1) Case One

During the unbalanced voltage dip, the negative-sequence currents flow from the inverter to the grid, causing unacceptable oscillation at the point of common coupling. This oscillation creates instability in the system. If the voltage dip issue at the point of common coupling is not considered while developing a control strategy for a wind power system, then the system may be disconnected from the grid. This case was studied by changing the voltage by 10% and 15% of the rated voltage for phases B and C respectively. Fig. 20 shows both active and reactive powers while changing the value of the grid voltage to

V_a = 110∠0, V_b= 110 * 0.9∠240, V_c= 110 * 0.85∠120

Clearly, the power oscillations at the output power increase owing to the effect of second-order harmonics and the double

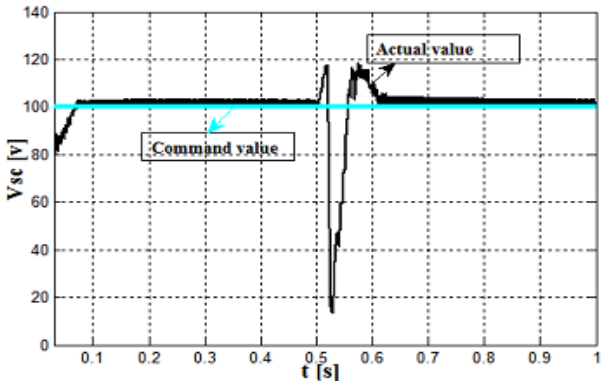

Fig. 16. Compensator voltage (V_{sc}) for the step change in speed.

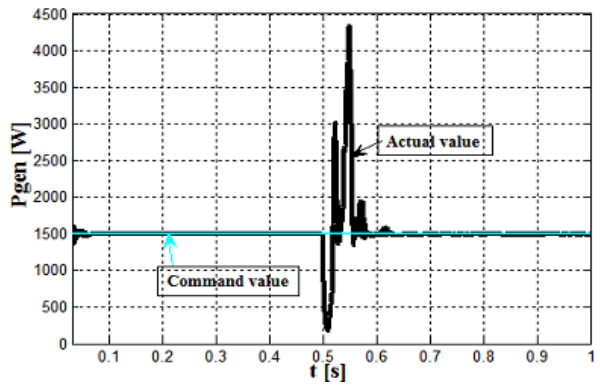

Fig. 17. Generator power (P_{gen}) for the step change in speed.

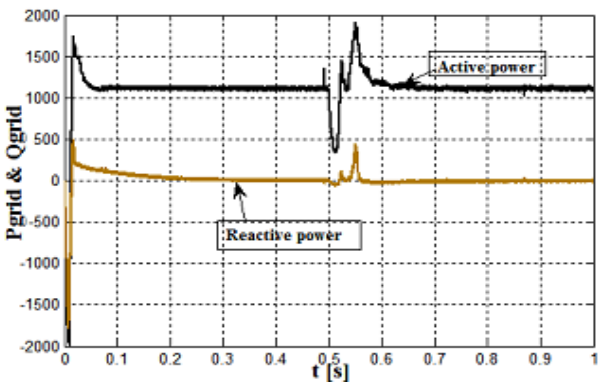

Fig. 18. Active and reactive powers injected to the grid for the step change in speed.

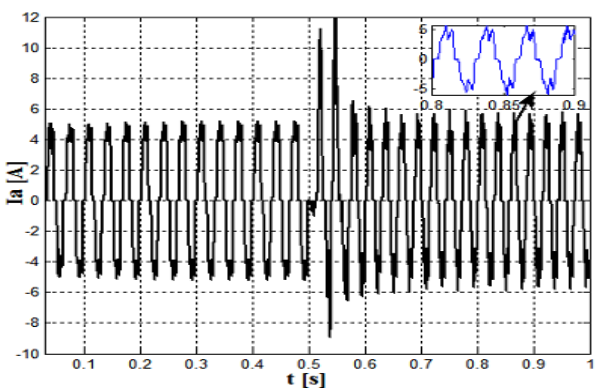

Fig. 19. Generator current for the step change in speed.

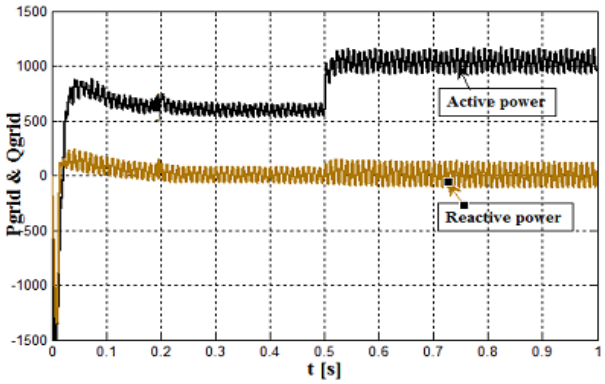

Fig. 20. Active and reactive powers of the grid while the value of the grid voltage is changed.

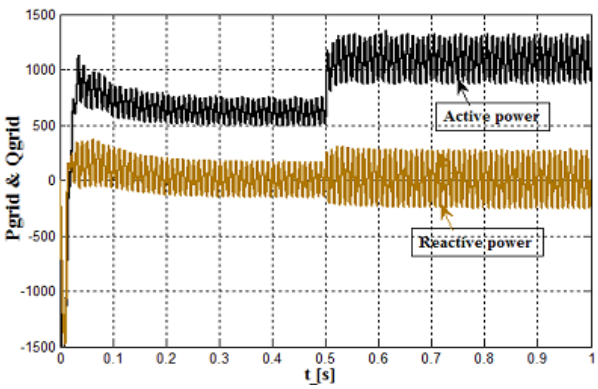

Fig. 21. Active and reactive powers of the grid while the phase voltage is changed.

frequency during the voltage dip.

2) Case Two

This case was studied by changing the voltage phase angle by 10% for phases B and C to V_a= 110∠0, V_b = 110 ∠216, V_c = 110 ∠132.

An unbalanced phase voltage will increase the peak current of the power converter in the same active and reactive power production. Fig. 21 shows the active and reactive powers of the grid while changing the phase voltage. Notably, in Fig. 21, the oscillations increased at the output power in the case of changing voltage phase angle. All calculations of power ripple and DC-link volt ripple are illustrated in Table III. These results prove the validity of the system to supply power management under small changes in voltage levels of the grid.

V. Experimental Work

The system shown in Fig. 22 is experimentally validated for the open loop system shown in Fig. 23(a) by using the TMSf28355 DSP, which is configured by the MATLAB/Simulink software. The two inverters are experimented by DSP with a switching frequency of 2.5 KHz. The vector sum of the compensator voltage and the generator voltage are rectified by using an uncontrollable full-wave rectifier bridge. To reduce the ripple content in the DC-link

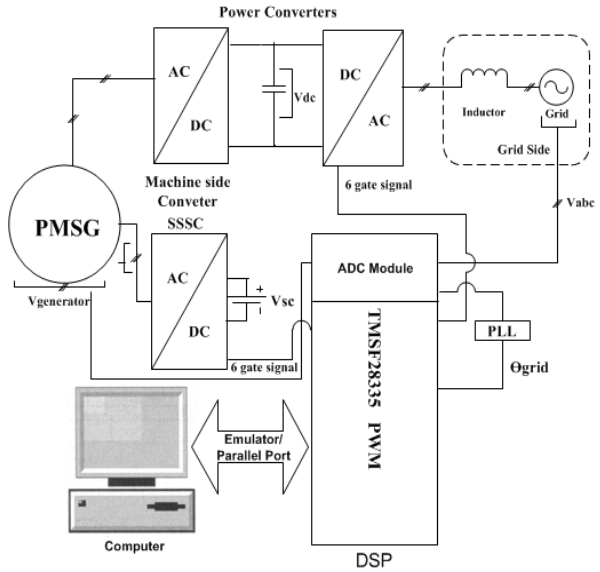

Fig. 22. Schematic of the experimental work.

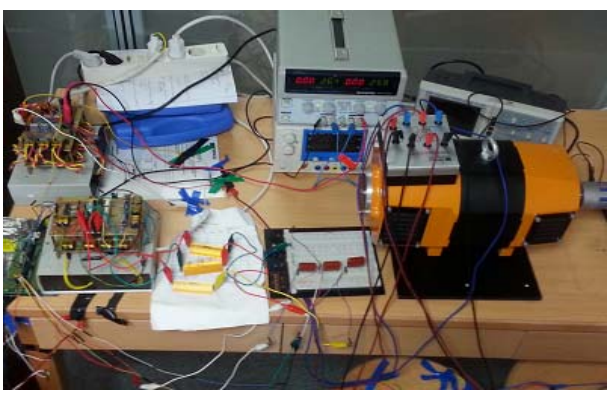

(a)

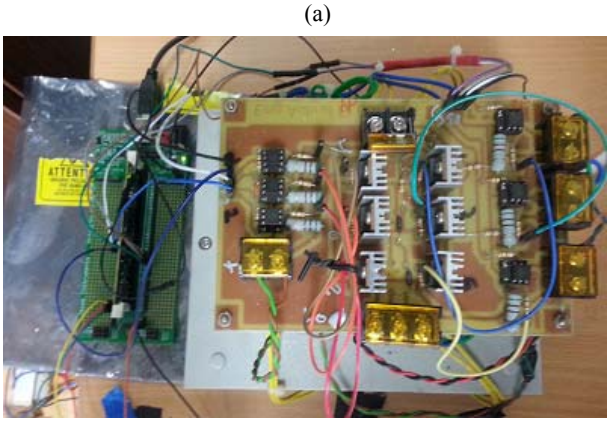

(b)

Fig. 23. (a) Overall rig (open winding generator, grid-side converter). (b) DC/AC Converter with DSP.

voltage, a 1000 µF, 400 V electrolytic capacitor is inserted between the rectifier output and the grid-side inverter. Fig. 24(a) shows the fundamental component of the compensator voltage versus the phase "A" of the generator voltage. Fig. 24(b) shows the generator voltage and the current of phase "A." Fig. 25 indicates the rectification voltage V_{dc}. Fig. 26(a) shows the fundamental component of this voltage versus the

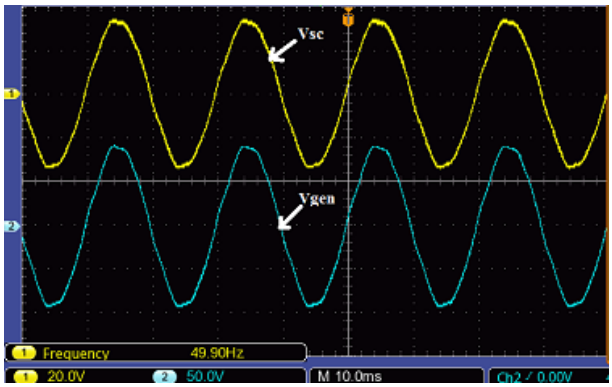

(a)

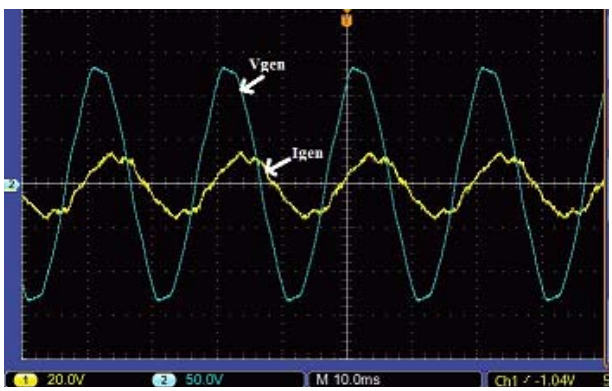

(b)

Fig. 24. Generator side. (a) The fundamental component of the compensator voltage versus the phase "A" of the generator voltage. (b) Generator voltage and current of phase "A."

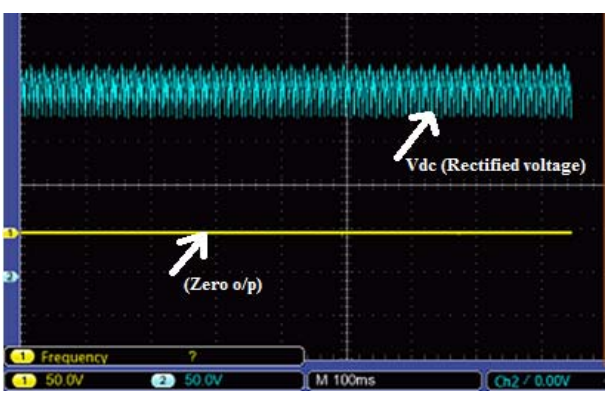

Fig. 25. DC Side: rectified voltage (V_{dc}).

phase "A" of the grid voltage. Fig. 26(b) represents the grid voltage and current of phase "A", and clearly shows that the phase "A" voltage and current are in phase. Accordingly, the reactive power is equal to zero.

On the basis of the above experimental results, the active and reactive powers at the generator side have values because the voltage leads the current, as shown in Fig. 27(b). At the DC side, the power can be calculated as $(V_{dc} * I_{dc})$. Injecting pure active power into the grid, as shown in Fig. 29(b), with the open loop control can be substituted in this equation to calculate the values of the V_{in} and theta $(\emptyset)$.

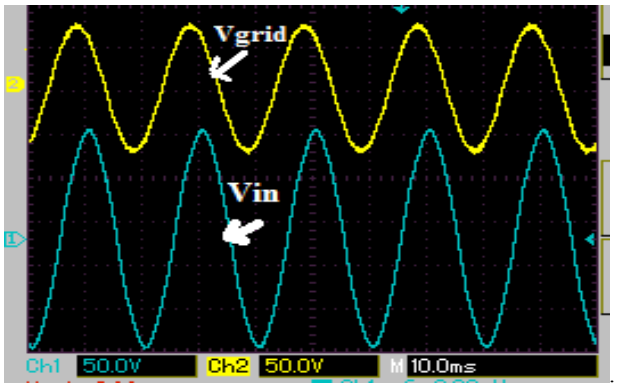

(a)

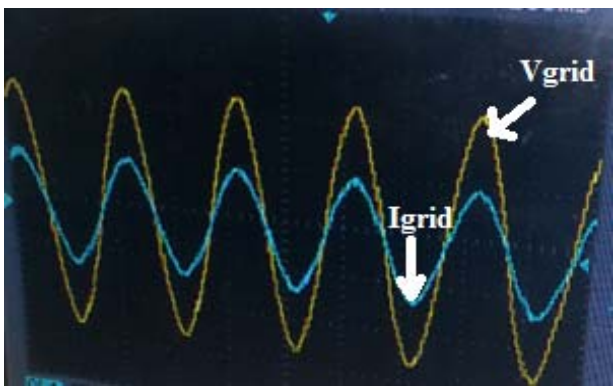

(b)

Fig. 26. Grid-side control: (a) the fundamental component of the grid inverter voltage versus the phase "A" of grid voltage; (b) grid voltage and current of phase "A."

$$V_{in}\angle\emptyset \;=\; I\angle 0\,(R + Jx_l) + V_{grid}\angle 0 \qquad (11)$$

The magnitude is used to determine the modulation index, and the theta is added to the firing angle to achieve power management requirements.

VI. Conclusion

Wind energy is a renewable energy that can be connected in an electrical network to meet increased load demands. In wind power applications, more attention is being focused on synchronous generators. The generator current and torque ripple have been improved by using a static synchronous series compensator. The proposed topology consists of an open-winding PMSG, which uses an uncontrolled diode rectifier and an auxiliary fractional-sized compensating VSI. Series compensation devices are used to counter the voltage drop on the synchronous reactance of the generator. This method is suitable for both constant- and variable-speed turbine systems. The overall system is verified through simulation and experimental work. The simulation is verified within two cases, namely, balanced and unbalanced line voltages. The obtained results show that the power system behavior associated with the series compensator is improved when the adjusted control system is applied to the verified model. The above simulation and experimental results also verify the validity of the system to satisfy all power management requirements under different voltage-level conditions.

References

[1] D. Pan and T. A. Lipo, "Series compensated open-winding PM generator wind generation system," *15th International Power Electronics and Motion Control, EPE-PEMC*, 2012.

[2] B. Wu, Y. Lang, N. Zargari, and S. Kouro, *Power Conversion and Control of Wind Energy Systems*, Wiley-IEEE Press, Hoboken, New Jersey, 2011.

[3] Y. G. Dessouky, "Journal of renewable energy and sustainable development," *Renewable Energy and Sustainable Development*, Vol. 1, No. 1, pp. 1-2, Aug. 2015. Available at: http://apc.aast.edu/ojs/index.php/RESD/article/view/01.1.001. Date accessed: 27 Oct. 2016.

[4] Z. Chen, J. M. Guerrero, and F. Blaabjerg, "A review of the state of the art of power electronics for wind turbines," *IEEE Trans. Power Electron.*, Vol.24, No.8, pp.1859-1875, Aug. 2009.

[5] J. A. Baroudi, V. Dinavahi, and A. M. Knight, "A review of power converter topologies for wind generators," *Electric Machines and Drives, 2005 IEEE International Conference on.*, pp. 458-465, 2005.

[6] M. F. Moussa, Y. G. Dessouky, and B. W. Williams, "Control strategy of a 6 MVA series connected synchronous generator for wind power," *IET Renewable Power Generation Conference*, *RPG 2011 of the IET,* 2011.

[7] A. Singer and W. Hofmann, "Static synchronous series compensation applied to small wind energy conversion system," *Power Electronics and Applications, European Conference on*, pp. 1-9, 2007.

[8] T. Takaku, G. Homma, T. Isober, S. Igarashi, Y. Uchida, and R. Shimada, "Improved wind power conversion system using magnetic energy recovery switch (MERS)," *Industry Applications Conference,. Fourtieth IAS Annual Meeting. Conference Record of the 2005*, Vol. 3, pp. 2007- 2012, Oct. 2005.

[9] B. Meghni, N. K. M'Sirdi, and A. Saadoun, "Maximum power tracking by VSAS approach for wind turbine, renewable energy sources," *Academy Publishing Center*, Vol. 1, No. 1, pp. 23-29, 2015.

[10] M. B. Smida and A..Sakly, "Pitch angle control for variable speed wind turbines," *Academy Publishing Center*, Vol. 1, No. 1, pp 81-88, 2015.

[11] R. Swisher, C. R. DeAzua, and J. Clendenin, "Strong winds on the horizon: Wind power comes of age," *Proc. IEEE*, Vol. 89, No. 12, pp. 1754-1764, Dec. 2001.

[12] D. Thakur, "Power Management Strategies for a Wind Energy Source in an Isolated Microgrid and Grid Connected System," University of Western Ontario - Electronic Thesis and Dissertation Repository, pp. 5-10, May 2015.

[13] R. A. Ibrahim, M. F. Moussa, Y. G. Dessouky, and B.W. Williams, "Parameters determination of grid connected interior permanent magnet synchronous generator," *EPE-PEMC ECCE Europe - 15th International Power Electronics and Motion Control Conference and Exposition*, 2012.

[14] A. Camacho, M. Castilla, J. Miret, and A. Borrell, "Reactive power control for distributed generation power plants to comply with voltage limits during grid faults," *IEEE Trans.*

Power Electron., Vol. 29, No. 11, pp. 6224-6234, Nov. 2014.
[15] D. Graovac, V. A. Kati, and A. Rufer, "Power quality problems compensation with universal power quality conditioning system," *IEEE Trans. Power Del*., Vol. 22, No. 2, pp. 968-976, Apr. 2007.
[16] M. F. Moussa and Y. G. Dessouky, "Design and control of a diode clamped multilevel wind energy system using a stand-alone AC-DC-AC converter," *Sustainability in Energy and Buildings conference*, 2012.
[17] F. Wang, J. L. Duarte, and M. A. M. Hendrix, "Grid interfacing converter systems with enhanced voltage quality for micro grid application – Concept and Implementation," *IEEE Trans Power Electron*., Vol. 26, No. 12, pp. 3501-3513, Dec. 2011.
[18] J. Miret, A. Camacho, M. Castilla, and J. Matas, "Control scheme with voltage support capability for distributed generation inverters under voltage sags," *IEEE Trans. Power Electron*., Vol. 28, No. 11, pp. 5252–5263, Nov. 2013.
[19] J. Miret, A. Camacho, M. Castilla, and J. Matas, "Voltage support control strategies for static synchronous compensators under unbalanced voltage sags," *IEEE Trans. Ind. Electron*., Vol. 61, No. 2, pp. 808-820, Apr. 2013.
[20] R. A. Ibrahim, M. S. Hamad, Y. G. Dessouky, and B. W. Williams, "A review on recent low voltage ride-through solutions of wind farm for permanent magnet synchronous generator," *SPEEDAM International Symposium on Power Electronics, Electrical Drives, Automation and Motion*, 2012.
[21] O. Elbeji, M. B. Hamed, and L. Sbita, "PMSG wind energy conversion system: Modelling and control," *International Journal of Modern Nonlinear Theory and Application*, pp. 88-97, Mar. 2014.
[22] A. T. Sohi, S. Javadi, and S. Z. Moussavi, "Energy management and power control for a grid-connected PMSG wind energy conversion system with extra function of harmonic elimination for local nonlinear loads," *Journal of Electrical and Electronics Engineering*, Vol. 9, No. 6, pp. 13-21, Ver. I, Nov./Dec. 2014.

Ashraf EL-Bardawil was born in Saudi Arabia. He received his BS and MS in Electrical Engineering from Arab Academy for Science, Technology, and Maritime Transport (AASTMT), Cairo, Egypt, in 2012 and 2016 respectively. Since 2012, he has been a teacher assistant at AAST. His current research interests are power electronics and control, which include AC machine drives and digital-signal-processing-based control applications.

Mona Fouad Moussa graduated from Alexandria University of Egypt in July 1998. Since 2004, she has worked in AASTMT as a Academic Dean of smart Village Campus. She received her PhD from Alexandria University in 2008. She has been an associate professor in the Department of Electrical and Control Engineering of the AASTMT since 2012. Currently, she is the head of the Engineering Departments in the College of Engineering and Technology in the AASTMT campus in Smart Village. She is a member of the IEEE, a consultant of multiple industrial companies, and a peer reviewer in numerous transactions, periodicals, and conferences. She was a member of the Organizing Committee of the "Development of Clean Energy Resources" workshop in May 2012 and the "Future of Hybrid Technology for Automotive Application" workshop sponsored by IEEE, IET, and NSF in the AASTMT, Egypt, in January 2011.